Did European temperatures in 1540 exceed present-day records?

2016 Environ. Res. Lett. 11 114021

(http://iopscience.iop.org/1748-9326/11/11/114021)

Environmental Research Letters

LETTER

Did European temperatures in 1540 exceed present-day records?

CrossMark

OPEN ACCESS

RECEIVED
8 September 2016

ACCEPTED FOR PUBLICATION
26 October 2016

PUBLISHED
15 November 2016

Rene Orth[1], **Martha M Vogel**[1], **Jürg Luterbacher**[2,3], **Christian Pfister**[4] **and Sonia I Seneviratne**[1]

[1] Institute for Atmospheric and Climate Science, ETH Zurich, Universitätstrasse 16, CH-8092 Zurich, Switzerland
[2] Justus Liebig University of Giessen, Department of Geography, Climatology, Climate Dynamics and Climate Change, Senckenbergstrasse 1, D-35930 Giessen, Germany
[3] Centre for International Development and Environmental Research, Justus Liebig University Giessen, Senckenbergstrasse 3, D-35390 Giessen, Germany
[4] Oeschger Centre for Climate Change Research, University of Bern, Falkenplatz 16, CH-3012 Bern, Switzerland

E-mail: rene.orth@env.ethz.ch **and** sonia.seneviratne@ethz.ch

Keywords: 1540 drought, climate model, soil moisture feedbacks, (extreme) temperature reconstruction

Supplementary material for this article is available online

Abstract

There is strong evidence that the year 1540 was exceptionally dry and warm in Central Europe. Here we infer 1540 summer temperatures from the number of dry days (NDDs) in spring (March–May) and summer (June–August) in 1540 derived from historical documentary evidence published elsewhere, and compare our estimates with present-day temperatures. We translate the NDD values into temperature distributions using a linear relationship between modeled temperature and NDD from a 3000 year pre-industrial control simulation with the Community Earth System Model (CESM). Our results show *medium confidence* that summer mean temperatures (T_{JJA}) and maximum temperatures (TXx) in Central Europe in 1540 were warmer than the respective present-day mean summer temperatures (assessed between 1966–2015). The model-based reconstruction suggests further that with a probability of 40%–70%, the highest daily temperatures in 1540 were even warmer than in 2003, while there is at most a 20% probability that the 1540 mean summer temperature was warmer than that of 2003 in Central Europe. As with other state-of-the-art analyses, the uncertainty of the reconstructed 1540 summer weather in this study is considerable, for instance as extrapolation is required because 1540-like events are not captured by the employed Earth system model (ESM), and neither by other ESMs. However, in addition to paleoclimatological approaches we introduce here an independent methodology to estimate 1540 temperatures, and contribute consequently to a reduced overall uncertainty in the analysis of this event. The characterization of such events and the related climate system functioning is particularly relevant in the context of global warming and the corresponding increase of extreme heat wave magnitude and occurrence frequency.

1. Introduction

Recent studies using instrumental and proxy climate information indicate that the 2003 European summer was likely the warmest for centuries (Luterbacher *et al* 2004, Schär *et al* 2004, Büntgen *et al* 2006, Dobrovolný *et al* 2010, Luterbacher *et al* 2016). The 2003 heat wave and drought caused severe impacts across various sectors (García-Herrera *et al* 2010) such as agriculture (Olesen *et al* 2011), public health (Fouillet *et al* 2006), or building infrastructure (Corti *et al* 2009). However, it remains unclear whether summer mean or maximum temperatures measured in 2003 exceeded any other very warm summer (comprising June, July and August, throughout this study) in previous centuries. This is because summer temperature reconstructions using documentary and natural proxy information include uncertainties due to unresolved variance in the statistical calibration period, an inhomogeneous distribution of proxies and a reduced number of climate information further back in time.

A particularly relevant year in this context is 1540 in which large parts of Europe experienced an exceptional multi-month drought and long-lasting warm conditions (Casty *et al* 2005, Pauling *et al* 2006, Wetter *et al* 2014, henceforth referred to as W14). Grape phenological evidence from Switzerland and the Czech Republic suggests that April to July temperatures in 1540 were possibly warmer than those in 2003 (Wetter and Pfister 2013, henceforth referenced to as W13, Mozný *et al* 2016). For almost the entire year the reported number of days with precipitation duly recorded by concerned chroniclers in Europe was very low. Overall precipitation amounts reconstructed from careful eye witness accounts in Switzerland and Poland were by far the lowest since 1500 (W14). The severity of the event is confirmed by river flow and wild fire records across continental Europe excluding Russia (W14).

The temperature reconstruction by W14 is not in line with statistical summer temperature estimations in eastern France (Chuine *et al* 2004) based on grape harvest dates. In this latter publication, 1540 summer temperature estimates are not particularly high. This is because at maturity the grapes were almost dried out so that vine-growers postponed the harvest until the next rain spell in late September (W13). According to a very long larch tree-ring series from an inner-alpine valley, the summer 1540 in the Alps was inferred as being even cool (Büntgen *et al* 2006) which might be attributable to the extreme drought (W13), because low growth normally associated with cold temperatures might have been induced instead by dry conditions in that year. The drought reconstructions by W14 were questioned by Büntgen *et al* (2015) who found no evidence of an exceptional drought in tree rings of various species at different locations across Europe. In response Pfister *et al* (2015) pointed out that tree-ring data may fail to show hot and dry outliers as comparisons during the instrumental period have confirmed. Moreover, the response of trees to extreme conditions is often lagged, which is also documented for 1540 (Büntgen *et al* 2011).

In this study we re-examine the question whether the 1540 summer was hotter than 2003 and present-day summer mean temperatures using climate model output. We present a novel and interdisciplinary approach which complements previous studies (W13, Pfister *et al* 2015, Mozný *et al* 2016) by providing an independent estimate of the (uncertain) 1540 temperatures. Combining paleoclimatology, global climate modeling and statistics, we estimate 1540 temperatures using the number of dry days (NDDs) reported by W14 together with an inferred relationship between NDD and temperatures from a simulation of pre-industrial climate in a state-of-the-art Earth system model (ESM). This analysis is based on the assumption that dry summers tend to be associated with more temperature extremes, as shown in models and observations for several hot summers (Seneviratne *et al* 2010, Hirschi *et al* 2011, Mueller and Seneviratne 2012, Whan *et al* 2015). With this approach we estimate temperature distributions that correspond with the observed 1540 NDD and compare these with present-day temperature means and with 2003 temperatures. This comparison allows us to infer probabilities that 1540 temperatures exceeded present-day mean and extreme values such as the 2003 summer.

2. Data

Addressing the question whether or not the 1540 summer temperatures exceeded that of present-day heat waves we analyze the relationship between NDD and summer temperatures from the simulation of 3000 years of pre-industrial climate of the community Earth system model (CESM, Gent *et al* 2011) version 1.2.2, which is a state-of-the-art ESM. For the simulations, all modules of the CESM were fully coupled: (i) atmosphere (Community Atmosphere Model version 4, Neale *et al* 2010), (ii) land (Community Land Model version 4, Oleson *et al* 2010), (iii) ocean (Parallel Ocean Program Version 2, www.cesm.ucar.edu/models/cesm1.1/pop2/doc/sci/POPRefManual.pdf (accessed on 16 March 2016)), and (iv) ice. In the land module also the carbon–nitrogen cycle is simulated, as well as ecosystem dynamics such that the vegetation can respond to environmental change. Note that the land model's dynamic vegetation mode is not activated in our simulations, i.e. plant species can not migrate into new regions or retreat from others. We use a spatial resolution of approximately 2° over land (1.9° × 2.5°) and approximately 1° over the oceans (gx1v6). The relationship between NDD and summer temperatures is based on the simulated land (soil moisture)-atmosphere (temperature) coupling characteristics of CESM. The land–atmosphere coupling in CESM displays a similiar temporal and spatial structure compared with other climate models, even though it is overall slightly weaker (Dirmeyer *et al* 2013, Seneviratne *et al* 2013).

From the NDD-temperature relationship we can infer 1540 temperatures using the NDD observed by chroniclers in 1540 across the Swiss Plateau (central northern Switzerland) and in Cracow (southern Poland) from W14. Note that W14 actually reported the number of wet days, whereas we use in this study the counterpart. These estimates are then compared with present-day temperatures from the gridded observation-based E-OBS dataset (Haylock *et al* 2008) version 12. We use a resolution of this dataset of 0.5° × 0.5° such that particular grid cells cover the Swiss Plateau, and also Cracow including its surroundings. The dataset provides daily mean and maximum temperatures from which we derive summer mean temperatures (T_{JJA}) and the maximum value of daily maximum temperatures (TXx). For comparison with the 1540 NDD records we also use precipitation from the E-OBS dataset to compute present-day NDD

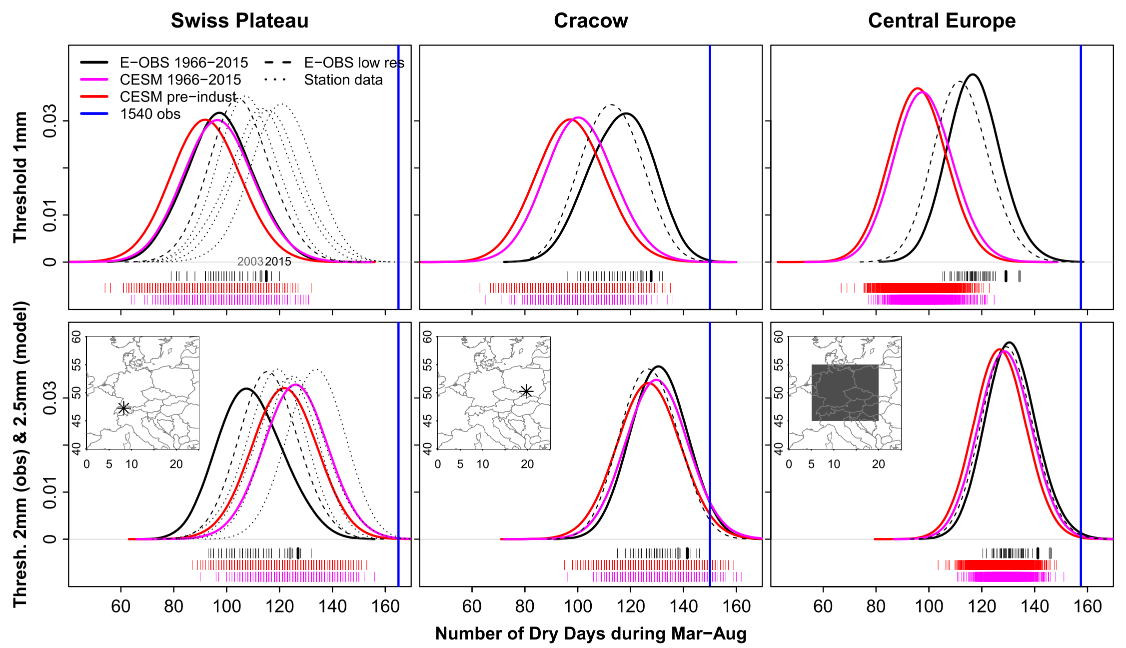

Figure 1. Distributions of NDD in different datasets at Swiss Plateau (left), Cracow (middle), and over the entire Central European domain. Results shown for 1 mm threshold in the top row, and for 2 mm (observations) and 2.5 mm (model) thresholds in the bottom row. Considered datasets include CESM model simulations with of pre-industrial climate (red) and of present-day climate (purple), gridded observations from E-OBS (black) and gauge observations from 4 sites located within the Swiss plateau (dotted black). Dashed black lines refer to E-OBS data aggregated to the same resolution as the CESM simulations. Estimates of 1540 NDD shown in blue.

estimates. Throughout this study we refer to 1966–2015 as the present-day time period.

Furthermore, we use a 21-member ensemble of transient CESM simulations covering the present-day period, computed in the same setup as described above. These simulations were re-started (branched) from the pre-industrial simulation and start in 1850. The individual ensemble members are re-started at least 20 years apart from one another to ensure different initial conditions and hence different realizations of the climate. In these simulations historical forcing of greenhouse gases, ozone and aerosols was used until 2005, and data from the RCP8.5 scenario from 2006 to 2015, as this scenario is most consistent with the current human emissions (Fuss *et al* 2014). Comparing this ensemble with the E-OBS temperatures we can compute the bias of CESM and correct the 1540 estimates accordingly (see section 3.2).

Data from the CESM simulations used in this study have been computed at ETH Zurich and are available upon request from Urs Beyerle (Beyerle, personal communication).

3. Methodology

The following subsections describe our methodology to infer possible 1540 temperature distributions that correspond with the observed NDD. Note that we cannot derive a single temperature value as different temperatures may occur even for similar NDD. The estimation of possible 1540 temperature distributions is done for the Swiss Plateau and Cracow separately using 3000 years of data from the pre-industrial CESM simulations. In addition to these two sites, we consider a Central European domain as there is evidence that the 1540 drought extended over this area (W14). This domain (45–55°N, 5–20°E) is determined from the area with most documentary evidence (figure 1 in W14), and it largely coincides with the Western European cluster in the classification established by Stefanon *et al* (2012). As there are no records of 1540 NDD from the whole domain we use the mean of the Swiss Plateau and Cracow observations. Even though the 1540 drought lasted from February until December we only consider the NDD from spring and summer (March until August) throughout this study as drought is expected to affect summer temperatures mostly in these seasons (Mueller and Seneviratne 2012, Orth and Seneviratne 2014).

As we are considering temperatures and NDD during different time periods, the inferred relationship between these variables (described below) includes two physical effects: (i) the large-scale (synoptic) weather situation which causes concomitant dry and warm conditions at the same time (Berg *et al* 2014), and (ii) soil moisture feedbacks which cause a lagged warming as dry soils can (persistently) limit evapotranspiration which consequently leads to increased sensible heat flux and temperatures. Note that the decreased evapotranspiration might cause secondary effects such as reduced cloud cover and consequently increased surface radiation which could intensify the initial warming induced by the soil moisture feedbacks.

3.1. Relationships of temperature versus NDD

We derive 1540 summer temperature estimates from the observed spring-summer NDD using the relationship between summer temperatures and spring-summer NDD simulated by CESM. In this context we consider T_{JJA} and TXx. These variables—in general and for a given NDD—follow different distributions, such that we use different approaches here to estimate the respective 1540 temperature distributions that correspond with the observed NDD at the different sites.

T_{JJA} follow a Gaussian distribution, hence we use a least-squares linear regression to capture the dependency on NDD as it assumes that the residuals follow a Gaussian distribution. With an ordinary linear regression, only the mean but not the variance of T_{JJA} is dependent on NDD. To address this shortcoming, we calculate the variance of T_{JJA} within 50 different quantile ranges (0%–2%, 2%–4%, ..., 98%–100%) and the corresponding 50 mean NDD estimates. We then perform a linear regression of this variance against the mean NDD. Note that this regression yields similar results when using other (regularly spaced) quantile ranges. With both linear regressions described above we can then use the observed NDD from 1540 to infer the mean and the variance of possible 1540 summer temperatures given the observed drought.

In contrast to T_{JJA}, TXx does not follow a Gaussian distribution. The values represent yearly maxima and can therefore be modeled with a generalized extreme value (GEV) distribution (Coles 2001). This is possible since all yearly values can be considered as independent and identically distributed (i.i.d.). Such a distribution is characterized by the location, scale and shape parameters, where the first two determine the expected value and the spread, respectively. To capture the role of NDD for these two parameters we fit a GEV to the 3000 TXx values from the CESM pre-industrial simulation and employ the 3000 respective NDD values as a covariate for the location and for the scale parameter (for another example employing a covariate in a TXx GEV fit, see Whan *et al* 2015). We use the likelihood ratio-test to confirm that NDD as a covariate for the two parameters significantly improves the GEV fit compared with corresponding GEV fits with no covariate or with NDD as a covariate in only the location or the scale parameter. Based on the described GEV and the observed 1540 NDD we can then infer location, scale and shape parameters of a possible 1540 TXx distribution. The respective assumed Gaussian and GEV distributions for summer mean temperatures and TXx, respectively, are confirmed with the Kolmogorov–Smirnov test (p-value < 0.05). All computations are done with the R statistical computing environment (R Core Team 2014), in particular with the 'extRemes' package (Gilleland and Katz 2011).

3.1.1. Uncertainty estimation

Uncertainties of the derived 1540 T_{JJA} and TXx distributions are inferred from the uncertainties in the underlying mean/location and variance/scale parameters for the Gaussian/GEV distributions. The uncertainties of these parameters are determined with bootstrapping. This means that from the 3000 simulation years used to infer the NDD-temperature relationship and consequently the parameters of the 1540 temperature distributions we draw random samples with replacement to reach the same sample size of 3000 years. From 300 such random 3000 year samples we compute 300 values for each parameter. From these 300 estimates we compute the 5% and 95% quantiles to yield a confidence range for each parameter. Using the 95% quantile of the mean/location and variance/scale parameters we obtain the hottest plausible 1540 temperature distribution at a particular site, and using the 5% quantiles of these parameters we derive the coldest possible temperature distributions. In the evaluation of the 1540 temperature distributions we focus on their hot tails to infer probabilities of exceeding present-day temperatures. Hence we only combine here low or high values for both parameters instead of using a high value for one parameter and a low value for the other (or vice versa), as this allows us to obtain the coldest or highest, respectively, hot tails in the resulting 1540 temperature distribution.

3.2. Correcting CESM temperature biases

We determine CESM's temperature bias by comparing present-day simulations with corresponding observations. Before assessing the bias we remove a linear trend from the data, because temperatures in the present-day period show clear warming trends, and differences in these trends between model data and observations could induce errors in the bias adjustment (Bellprat *et al* 2013). As the T_{JJA} and TXx data follow different distributions, we employ different approaches to adjust the respective biases. Biases in T_{JJA} are addressed by adjusting the mean and the variance (standard deviation) of the present-day simulations to the values of the corresponding observations, while biases in TXx are addressed through a quantile mapping procedure (Gudmundsson *et al* 2012) where the shape of the GEV distribution of the modeled TXx is adjusted to the shape of the GEV distribution of the observations. Assuming that CESM has identical biases in the pre-industrial and detrended present-day simulations, the same adjustments are applied to correct the biases in the derived 1540 temperature distributions. The bias adjustment is applied separately at all considered sites, and for T_{JJA} and TXx. This means that we directly bias-correct the temperature indices used in this study instead of the underlying daily temperatures. After this bias adjustment, we can unambiguously compare the inferred model-based 1540 temperatures with present-day temperature observations.

Note that as in the CESM temperature estimates, there might also be a bias in the modeled NDD. This will be addressed by applying different precipitation thresholds to distinguish between wet and dry days in section 4.1. Biases in temperature and NDD might be related and should be corrected together in this case. Nevertheless we chose to apply simple, individual bias corrections instead of a more sophisticated procedure. The reason for this is that the temperature biases were found to be constant across summers with different NDD, and similarly the NDD biases were found to be similar in summers with different temperatures, indicating limited interaction between the biases of the two quantities (not shown).

4. Results

4.1. Comparing 1540 NDD with CESM simulations and present-day observations

In a first step we compare the NDD recorded in 1540 with NDD obtained from E-OBS and the CESM simulations in figure 1. As mentioned before we consider the Swiss Plateau and Cracow sites as well as a Central European domain. In the upper row we apply the 1 mm daily precipitation threshold used in W14 to distinguish dry from wet days and find that the recorded 1540 NDD lie far outside the NDD distributions derived from CESM and E-OBS. For comparison we show E-OBS NDD values from the 2003 drought (Schär *et al* 2004) and the 2015 drought (Orth *et al* 2016). There is an increase of NDD from pre-industrial to present-day climate in the CESM simulations, however, NDD in the present-day simulation are clearly lower than in E-OBS. This bias can be explained by three different effects. One possible reason is the different spatial resolution of CESM (2°) and E-OBS (0.5°), which likely also contributes to the temperature bias (see section 3.2). The dotted lines in the Swiss Plateau results represent NDD from station data from the same cities from which the 1540 observation for this area was derived (Basle, Lucerne, Winterthur, Zurich). They underline that the NDD increases at lower spatial scales. Similarly, upscaling the E-OBS data to the CESM spatial resolution (dashed lines) through spatial averaging generally leads to less NDD, except at the Swiss Plateau as the upscaling leads to the inclusion of Alpine areas with high NDD. Hence the spatial scale mismatch may also explain part of the offset between the point-scale 1540 observations and the other data. However, an offset remains even between the NDD of the upscaled E-OBS and of the CESM present-day data. This remaining difference is probably due to the precipitation undercatch in the E-OBS data (Hofstra *et al* 2009), where the underestimation of actual precipitation leads to higher NDD. Furthermore it could be related to biases in the precipitation simulated by CESM.

In the lower row of figure 1 higher precipitation thresholds are applied to yield NDD distributions closer to the 1540 observations. For the E-OBS data a lower threshold is used than for the CESM data to compensate for the precipitation undercatch, and possible precipitation biases in CESM. This results in good agreement between NDD in the present-day CESM simulations and in E-OBS. Only few differences remain at the Swiss Plateau, possibly due to the mountain influence. Hence, the application of the different thresholds successfully corrects the NDD bias of the CESM model described above. Furthermore, the different spatial scales appear to be less important for the higher thresholds, such that e.g. the original and upscaled E-OBS NDD are more comparable. This effect, and the higher threshold itself which accounts for the undercatch in observed precipitation, move the range of the CESM pre-industrial NDD closer to the 1540 NDD observations, and consequently make the model data and the paleoclimatological reconstruction (more) comparable. The fact that the 1540 NDD observations is close to the maxima of the CESM pre-industrial NDD allows us to jointly analyze these data in order to derive corresponding temperature estimates, consequently the NDD estimates derived with higher threshold(s) will be used in the following analyses. Note, however, for both thresholds the 1540 NDD is slightly outside the range of the other considered data (except for the higher threshold at Cracow) which underlines the exceptional magnitude of the 1540 drought and suggests that it was worse than any present-day drought in Central Europe. Because of the ongoing global warming it is not clear if also the corresponding temperatures exceeded present-day records. This will be analyzed in the following section.

4.2. Estimation of 1540 temperatures

Figure 2 displays the relationships between temperatures and NDD in the CESM pre-industrial data. All regression slopes are significantly different from zero. The slopes are higher for TXx than for T_{JJA}, i.e. the relationships are stronger. This is in line with earlier results generally reporting larger effects of dry soils on temperature extremes than on mean temperatures (Seneviratne *et al* 2013, Hauser *et al* 2016, Orth and Seneviratne 2016). Beside the temperature increase towards a higher NDD, also the temperature variability increases. This is illustrated with quantile regressions in figure 2, and needs to be accounted for in the estimation of the 1540 temperature distributions. Note that they are only used for illustration purposes here and not employed in the estimation of 1540 temperature distributions. As discussed in section 3.1, in the case of TXx the 1540 temperature distributions are estimated by considering NDD as a covariate for

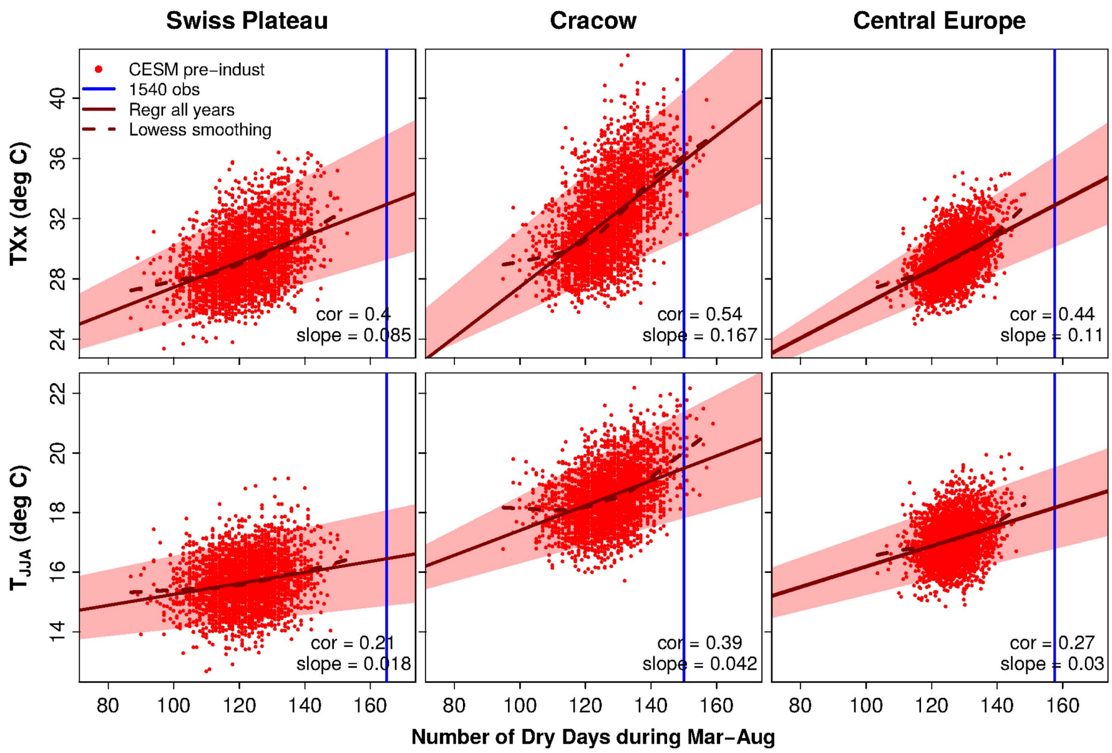

Figure 2. Relationships between summer maximum (top) and mean (bottom) temperatures and NDD in CESM pre-industrial simulations. Dark red lines show least-squares regression fits (solid line) and lowess smoother (dashed line). Shaded area is determined by quantile regressions using the 5% (lower bound) and 95% (upper bound) quantiles. Estimates of NDD in 1540 shown in blue.

the scale parameter when fitting the GEV, and in the case of T_{JJA} this is done by fitting linear dependencies between the temperature variability and NDD.

The validity of the linearity between temperature and NDD that is assumed here is tested with lowess smoothing (Cleveland 1982) fits which are displayed as dashed lines. This smoothing is based on locally weighted polynomial regression, and we employ a smoothing span of 1/3, i.e. at each value the smooth is influenced by the surrounding 1/3 of all data points. For most of the NDD range the fits correspond well with the linear relationships, confirming the linearity assumption. Weaker relationships are found coherently in wet conditions (smaller slope towards low NDD), while the relationships are generally stronger in dry conditions (increased slope towards high NDD). This suggests a stronger (weaker) impact of NDD on temperatures under dry (wet) conditions. This is likely due to the role of soil moisture feedbacks: Central Europe is usually in a humid regime, where evapotranspiration is energy-limited. However, in dry summers evapotranspiration can become soil moisture-limited instead. In this case evapotranspiration decreases towards higher NDD, and at the same time the sensible heat flux and consequently the surface temperature increases. At even higher NDD evapotranspiration will get close to zero, and as it can not decrease further the temperature increase will slow down. Hence the stronger NDD-temperature relationships we observe in figure 2 are expected to weaken towards even drier conditions (even more NDD) as in the 1540 summer. In other words, while the 1540 temperature distributions we estimate from the regression considering all years tend to be rather conservative estimates, we would overestimate the 1540 temperature distribution when considering only dry years in the regression as the resulting higher slopes are only observed within a limited, so-called transitional soil moisture range.

The modeled NDD-temperature relationships are key to infer the 1540 temperature distributions and hence for the conclusions of this study. We validate them by comparing the slopes across the CESM simulations and E-OBS observations in figure S1. A linear detrending of the present-day data is performed; for the CESM simulations the mean linear trend across all ensemble member is removed. Different slopes are found before and after detrending the present-day data underlining the role of the temperature and NDD trends, and the importance to detrend the data before comparing them with pre-industrial simulations. Therefore, we focus on the results derived with detrended data here. There are no statistically significant differences between the pre-industrial and present-day slopes in CESM suggesting that climate change did not (yet) effect this relationship. More importantly, the present-day slopes in the CESM data are similar to the slopes computed from observations, there are no statistically significant differences except for TXx at Cracow. The observed slopes overall tend to be slightly

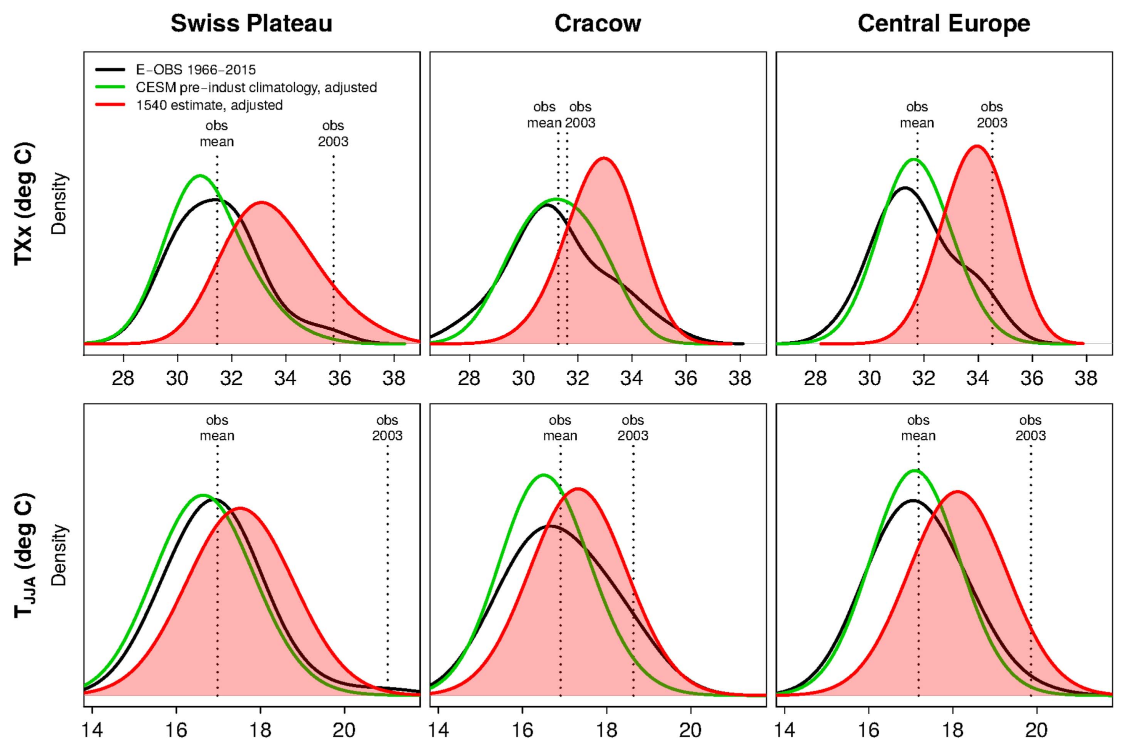

Figure 3. Distributions of summer maximum (top) and mean (bottom) temperatures in observations, bias-corrected pre-industrial CESM simulations and bias-corrected 1540 estimates as inferred from the relationships in figure 2. Dotted lines denote mean observed temperatures, and 2003 temperatures.

larger than the CESM present-day slopes in the case of T_{JJA}, and slightly lower in the case of TXx. Overall these results indicate that CESM successfully captures the temperature-NDD relationship operating in nature such that we can use its pre-industrial simulations to infer 1540 temperatures through this statistical relationship.

Before inferring the 1540 temperatures by applying the statistical methodology described in sections 3.1 and 3.2, we test this methodology by estimating present-day temperatures. The resulting reconstruction is compared with observations in figure S2. The validation is deemed successful, because as expected about half of the observed values are within the reconstructed 25–75th percentile range, and the majority of the values are within the reconstructed 5–95th percentile range. Furthermore, for particularly warm summers across the Central European domain such as 2003, 1992 and 1983, the reconstructed temperature distribution is shifted towards warmer conditions. While there is considerable year-to-year variability in the reconstructed temperatures for Central Europe, there is almost none for TXx at Cracow. This is due to the weak and insignificant underlying temperature-NDD relationship shown in figure S1. Note that this problem does not affect the estimation of the 1540 temperatures as the temperature-NDD relationships for the pre-industrial climate are estimated from much larger samples (3000 years instead of 50) such that the estimated relationships are more accurate and significant for all considered regions and temperature metrics. Another interesting feature is the higher year-to-year variability at the upper end of the reconstructed temperature distribution compared with that at the lower end. This is in correspondence with the observations (strongest outliers are found at hot conditions) and can be explained with the increasing variability of temperature towards drier conditions which is illustrated in figure 2. Overall, these results highlight the applicability of our methodology, in particular for extreme events such as the 1540 summer.

Performing this analysis, we derive the bias-adjusted temperature distributions that correspond to the 1540 NDD observations as shown in figure 3. Not surprisingly they are clearly warmer than the overall bias-adjusted CESM pre-industrial temperatures underlining the role of the high NDD. As main result of this study, we find that the 1540 temperature distributions are also warmer than present-day temperature distributions at all sites and for both TXx and T_{JJA}. Furthermore it can not be excluded that 1540 was hotter than 2003. However, these results of course depend on the threshold employed in the NDD computation. This is investigated further in the next section.

4.3. Role of precipitation threshold used in NDD computation

From the results in figure 2 we can infer the likelihood of 1540 temperatures exceeding present-day mean temperatures or 2003 temperatures. These probabilities were computed for different precipitation

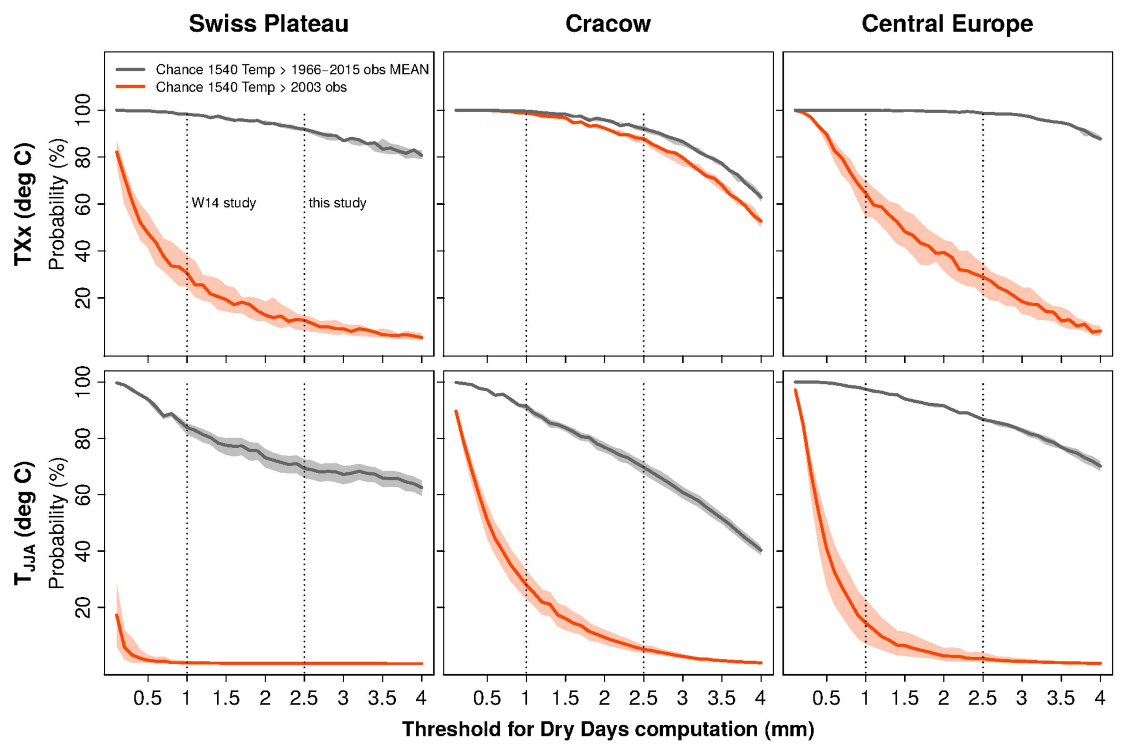

Figure 4. Estimated probabilities of 1540 summer maximum (top) and mean (bottom) temperatures exceeding present-day values for different thresholds used in the NDD computation. Probabilities for exceeding observed mean temperatures are shown in gray, probabilities for exceeding 2003 values are shown in orange.

thresholds used in the NDD computation between 0.1 and 4 mm. The results are shown in figure 4. They allow us to quantify the main result of this study: we find that overall the probabilities that 1540 temperatures exceeded present-day means of T_{JJA} or TXx in the Swiss Plateau and Cracow are rather high (70%–100% or 80%–100% chance for the thresholds used in this study and in W14, respectively). Focusing on 2003 as a present-day extreme event we find that generally low probabilities that 1540 temperatures were hotter (0%–10% or 0%–30% chance for the threshold used in this study and in W14, respectively), except for TXx at Cracow for which probabilities are high (almost 100% or 80% chance for the threshold used in this study and in W14, respectively, respectively) which is because the 2003 TXx was not exceptional in this location. For the entire Central European region we also find high probabilities that 1540 T_{JJA} and TXx exceeded corresponding present-day mean values, but low probabilities that they exceeded the 2003 values. Our confidence in the Central European results is slightly lower than for the Swiss Plateau and Cracow results because the underlying NDD was estimated from these two point observations.

Note that even though the 2003 summer is widely used as a benchmark for hot extremes, some of the present-day extreme values may have been recorded in summers other than in 2003, dependent on the considered location and temperature metric. Focusing on the location- and metric-dependent present-day extremes instead of the 2003 values, however, we find similar results as shown in figure S3. The results are identical at the Swiss Plateau and in the case of T_{JJA} across Central Europe because the 2003 values are the most extreme throughout the present-day period. In the case of TXx at Cracow we find the largest difference because 2003 TXx were not particularly extreme at this location, as mentioned above.

As the impact of NDD is stronger on extreme temperatures there are generally higher probabilities of exceeding present-day TXx rather than T_{JJA}. All probability curves are decreasing with increasing threshold as the resulting NDD in the CESM pre-industrial simulations increases and hence the 1540 NDD observations are less extreme and so are the inferred corresponding temperature distributions. The shadings in figure 4 represent the 5%–95% uncertainty range (see section 3.1.1). Thanks to the large 3000 year length of the pre-industrial CESM simulation the uncertainties are overall rather small.

5. Conclusions

In this study, we investigate the probability that the 1540 summer was warmer than the extreme 2003 summer, and than average summers in the past 5 decades. For this purpose, we use an approach relating the reported spring-summer NDD to summer temperatures (T_{JJA}) and temperature extremes (TXx) using climate model simulations.

Based on these analyses, we can state that our results confirm that the large drought reported in 1540 also implied above-average summer temperatures in Central Europe that summer, as suggested by W14. This result is relevant for the dendrochronological community, since most tree-ring records do not show outstanding features in that year (Büntgen *et al* 2015, Pfister *et al* 2015). It is more difficult to assess if the summer in 1540 was warmer than in 2003, which was the warmest Central European summer in the observational record (Schär *et al* 2004, Luterbacher *et al* 2016). Our model results suggest a rather high probability that this was the case for TXx (~40%–70%), but a lower probability (~5%–10%) for T_{JJA}. However this hypothesis cannot be excluded.

We successfully validated our approach to the extent possible by comparing the NDD-temperature relationships between observations and climate model simulations, and by applying the methodology to estimate present-day temperatures, but some underlying uncertainties in the derivation of the 1540 temperature distributions remain. These include (1) the reliability of the historical (NDD) records and their low geographical coverage, (2) the dependency of the results on simulations with a single climate model, (3) the fact that the historical reported 1540 NDD numbers exceed by far the maximum NDD simulated in the model for the relevant historical time period (as is the case in other climate models, W14). Given these uncertainties, we assess that quantitative results from our study should be considered with *medium confidence* consistently with IPCC uncertainty language (e.g. Mastrandrea *et al* 2010, Seneviratne *et al* 2012).

These uncertainties, and the similarly large uncertainties in other reconstructions of the 1540 temperatures (W13, Pfister *et al* 2015), thus highlight the need for more detailed analyses of the exact conditions that prevailed in 1540. This interdisciplinary analysis is a step in this direction. Besides the actual 1540 summer temperature estimates summarized above we present an independent approach to obtain these results by combining paleoclimatological reconstructions with ESM simulations to assess past climate conditions. Together with previous estimates and additional future analyses, this contributes to reduce the overall uncertainty in the description of a possibly benchmark-setting extreme event. The characterization of such a summer, and of the overall climate system functions under these extreme conditions is especially important in the context of global warming whereby the accelerated warming of hot temperatures over land (Seneviratne *et al* 2016) might lead to a regular recurrence of such extreme events.

Acknowledgments

We thank Nico Kröner and Randal Koster for helpful discussion on the methodology, Jakob Zscheischler for statistical advice, and Urs Beyerle for access to and help with the CESM simulations. We acknowledge the E-OBS dataset established by the EU-FP6 project ENSEMBLES (http://ensembles-eu.metoffice.com (accessed on 18 March 2016)) and the data providers in the ECA&D project (www.ecad.eu (accessed on 18 March 2016)) for providing precipitation and temperature data. We also acknowledge funding from the European Union's Seventh Framework Programme (FP7/2007-2013) under grant agreement no 607085 (EUCLEIA) and the European Research Council (ERC) under grant agreement no 617518 (DROUGHT–HEAT).

References

Bellprat O, Kotlarski S, Lüthi D and Schär C 2013 Physical constraints for temperature biases in climate models *Geophys. Res. Lett.* **40** 1–6

Berg A, Lintner B, Findell K, Malyshev S, Loikith P and Gentine P 2014 Impacts of soil moisture-atmosphere interactions on surface temperature distribution *J. Clim.* **27** 7976–93

Büntgen U, Brazdil R, Heussner K-U, Hofmann J, Kontic R, Kyncl T, Pfister C, Chroma K and Tegel W 2011 Combined dendro-documentary evidence of central European hydroclimatic springtime extremes over the last millennium *Quat. Sci. Rev.* **30** 3947–59

Büntgen U, Frank D C, Nievergelt D and Esper J 2006 Summer temperature variations in the European Alps, A.D. 755–2004 *J. Clim.* **19** 5606–23

Büntgen U, Tegel W, Carrer M, Krusic P J, Hayes M and Esper J 2015 Commentary to Wetter *et al* (2014): limited tree-ring evidence for a 1540 European Megadrought *Clim. Change* **131** 183–90

Casty C, Wanner H, Luterbacher J, Esper J and Böhm R 2005 Temperature and precipitation variability in the European Alps since 1500 *Int. J. Climatol.* **25** 1855–80

Chuine I, Yiou P, Viovy N, Seguin B, Daux V and Ladurie E L R 2004 Historical phenology: grape ripening as a past climate indicator *Nature* **432** 289–90

Cleveland W S 1982 LOWESS: a program for smoothing scatterplots by robust locally weighted regression *Am. Stat.* **35** 54

Coles S 2001 *An Introduction to Statistical Modeling of Extreme Values* (Berlin: Springer)

Corti T, Muccione V, Köllner-Heck P, Bresch D and Seneviratne S I 2009 Simulating past droughts and associated building damages in france *Hydrol. Earth Syst. Sci.* **13** 1739–47

Dirmeyer P A, Kumar S, Fennessy M J, Altshuler E L, DelSole T, Guo Z, Cash B A and Straus D 2013 Model estimates of land-driven predictability in a changing climate from CCSM4 *J. Clim.* **26** 8495–512

Dobrovolný P *et al* 2010 Monthly, seasonal and annual temperature reconstructions for Central Europe derived from documentary evidence and instrumental records since AD 1500 *Clim. Change* **101** 61–107

Fouillet A, Rey G, Laurent F, Pavillon G, Bellec S, Guihenneuc-Jouyaux C, Clavel J, Jougla E and Hémon D 2006 Excess mortality related to the August 2003 heat wave in france *Int. Arch. Occup. Environ. Health* **80** 16–24

Fuss S *et al* 2014 Betting on negative emissions *Nat. Clim. Change* **4** 850–3

García-Herrera R, Díaz J, Trigo R M, Luterbacher J and Fischer E 2010 A review of the European summer heat wave of 2003 *Crit. Rev. Environ. Sci. Technol.* **40** 267–306

Gent P R *et al* 2011 The community climate system model version 4 *J. Clim.* **24** 4973–91

Gilleland E and Katz R W 2011 New software to analyze how extremes change over time *Eos Trans. Am. Geophys. Union* **92** 13–4

Gudmundsson L, Bremnes J B, Haugen J E and Engen-Skaugen T 2012 Technical note: downscaling RCM precipitation to the station scale using statistical transformations—a comparison of methods *Hydrol. Earth Syst. Sci.* **16** 3383–90

Hauser M, Orth R and Seneviratne S I 2016 Role of soil moisture vs. recent climate change for heat waves in western Russia *Geophys. Res. Lett.* **43** 2819–26

Haylock M R, Hofstra N, Tank A K, Klok E, Jones P and New M 2008 A European daily high-resolution gridded dataset of surface temperature and precipitation *J. Geophys. Res.* **113** 119

Hirschi M, Seneviratne S I, Alexandrov V, Boberg F, Boroneant C, Christensen O B, Formayer H, Orlowsky B and Stepanek P 2011 Observational evidence for soil-moisture impact on hot extremes in southeastern Europe *Nat. Geosci.* **4** 17–21

Hofstra N, Haylock M, New M and Jones P D 2009 Testing E-OBS European high-resolution gridded data set of daily precipitation and surface temperature *J. Geophys. Res.* **114** 101

Luterbacher J, Dietrich D, Xoplaki E, Grosjean M and Wanner H 2004 European seasonal and annual temperature variability, trends and extremes since 1500 *Science* **303** 1499–503

Luterbacher J *et al* 2016 European summer temperatures since Roman times *Env. Res. Lett.* **11** 024001

Mastrandrea M D 2010 Guidance note for lead authors of the IPCC fifth assessment report on consistent treatment of uncertainties *Technical Report* Intergovernmental Panel on Climate Change (IPCC) (www.ipcc.ch/pdf/supporting-material/uncertainty-guidance-note.pdf)

Mozný M, Brázdil R, Dobrovolný P and Trnka M 2016 April–August temperatures in the Czech Lands, 1499–2015, reconstructed from grape-harvest dates *Clim. Past* **12** 1421–34

Mueller B and Seneviratne S I 2012 Hot days induced by precipitation deficits at the global scale *Proc. Natl Acad. Sci.* **109** 12398–12403

Neale R B, Richter J H, Conley A J, Park S, Lauritzen P H, Gettelman A and Williamson D L 2010 Description of the NCAR community atmosphere model (CAM 4.0) *NCAR Technical Note* NCAR/TN-485+STR (www.ccsm.ucar.edu/models/ccsm4.0/cam/docs/description/cam4_desc.pdf)

Olesen J E, Trnka M, Kersebaum K C, Skjelvågd A O, Seguine B, Peltonen-Sainiof P, Rossig F, Kozyrah J and Micalei F 2011 Impacts and adaptation of European crop production systems to climate change *Eur. J. Agron.* **34** 96–112

Oleson K W 2010 Technical description of version 4.0 of the community land model (CLM) *NCAR Technical Note* NCAR/TN-478+STR (www.cesm.ucar.edu/models/cesm1.0/clm/CLM4_Tech_Note.pdf)

Orth R and Seneviratne S I 2014 Using soil moisture forecasts for sub-seasonal summer temperature predictions in Europe *Clim. Dyn.* **43** 3403–18

Orth R and Seneviratne S I 2016 Variability of soil moisture and sea surface temperatures similarly important for land climate in the warm season in the community Earth system model *J. Clim.* (in review)

Orth R, Zscheischler J and Seneviratne S I 2016 Record dry summer in 2015 challenges precipitation projections in Central Europe *Sci. Rep.* **6** 28334

Pauling A, Luterbacher J, Casty C and Wanner H 2006 500 years of gridded high-resolution precipitation reconstructions over Europe and the connection to large-scale circulation *Clim. Dyn.* **26** 387–405

Pfister C *et al* 2015 Tree-rings and people—different views on the 1540 Megadrought. Reply to Büntgen *et al* 2015 *Clim. Change* **131** 191–8

R Core Team 2014 *R: A language and environment for statistical computing* R Foundation for Statistical Computing, Vienna, Austria(www.R-project.org/)

Schär C, Vidale P L, Lüthi D, Frei C, Häberli C, Liniger M and Appenzeller C 2004 The role of increasing temperature variability in European summer heat waves *Nature* **427** 332–6

Seneviratne S I, Corti T, Davin E L, Hirschi M, Jaeger E B, Lehner I, Orlowsky B and Teuling A J 2010 Investigating soil moisture–climate interactions in a changing climate: a review *Earth-Sci. Rev.* **99** 125–61

Seneviratne S I, Donat M, Pitman A J, Knutti R and Wilby R L 2016 Allowable CO_2 emissions based on regional and impact-related climate targets *Nature* **529** 477–83

Seneviratne S I 2012 Changes in climate extremes and their impacts on the natural physical environment *Managing the Risks of Extreme Events and Disasters to Advance Climate Change Adaptation, A Special Report of Working Groups I and II of the Intergovernmental Panel on Climate Change (IPCC)* pp 109–230 (www.ipcc.ch/pdf/special-reports/srex/SREX-Chap3_FINAL.pdf)

Seneviratne S I *et al* 2013 Impact of soil moisture-climate feedbacks on CMIP5 projections: first results from the GLACE-CMIP5 experiment *Geophys. Res. Lett.* **40** 5212–7

Stefanon M, D'Andrea F and Drobinski P 2012 Heatwave classification over Europe and the mediterranean region *Env. Res. Lett.* **7** 1–9

Wetter O and Pfister C 2013 An underestimated record breaking event—why summer 1540 was likely warmer than 2003 *Clim. Past* **9** 41–56

Wetter O *et al* 2014 The year-long unprecedented European heat and drought of 1540—a worst case *Clim. Change* **125** 349–63

Whan K, Zscheischler J, Orth R, Shongwe M, Rahimi M, Asare E and Seneviratne S I 2015 Impact of soil moisture on extreme maximum temperatures in Europe *WACE* **9** 57–67